Research Article

Nano Research
2020, 13(10): 2658–2664

ISSN 1998-0124 CN 11-5974/O4
https://doi.org/10.1007/s12274-020-2907-5

Tunable colors and conductivity by electroless growth of Cu/Cu_2O particles on sol-gel modified cellulose

Justus Landsiedel[1] (✉), Waleri Root[1], Christian Schramm[1], Alexander Menzel[2], Steffen Witzleben[3], Thomas Bechtold[1], and Tung Pham[1] (✉)

[1] *Research Institute for Textile Chemistry and Textile Physics, University of Innsbruck, 6850 Dornbirn, Austria*
[2] *Department of Physical Chemistry, University of Innsbruck, 6020 Innsbruck, Austria*
[3] *Department of Natural Sciences, Bonn-Rhein-Sieg University of Applied Sciences, 53359 Rheinbach, Germany*

Received: 4 March 2020 / **Revised:** 27 May 2020 / **Accepted:** 29 May 2020

ABSTRACT

Development of colored surfaces by formation of nano-structured aggregates is a widely used strategy in nature to color lightweight structures (e.g. butterflies) without the use of dye pigments. The deposition of nanoscale particles mimics nature in it's approach coloring surfaces. This work presents sol-gel modification of cellulose surfaces used to form a template for growth of Cu/Cu_2O core–shell particles with defined size-distributions. Besides improving the adhesion of the deposited particulate material, the sol-gel matrix serves as a template for the control of particle sizes of the Cu/Cu_2O structures, and as a consequence of particle size variation the surface color is tunable. As an example, red color was achieved with an average particle size of 35 nm, and shifts gradually to blue appearance when particles have grown to 80 nm on the sol-gel modified fabric. The copper concentration on representative fabrics is kept low to avoid modifying the textile characteristics and were all in the range of 150–170 mg per g of cellulose material. As a result of copper deposition on the surface of the material, the cellulose fabric also became electrically conductive. Remarkably, the electrical conductivity was found to be dependent on the average particle sizes of the deposits and thus related to the change in observed color. The generation of color by growth of nano-sized particles on sol-gel templates provides a highly promising approach to stain surfaces by physical effects without use of synthetic colorants, which opens a new strategy to improve environmental profile of coloration.

KEYWORDS

electroless copper deposition, sol-gel support, thin film, structural coloration, tunable sheet resistance, LSPR

1 Introduction

Structurally induced coloration is a phenomenon that is often associated with naturally occurring nanoscale structures, which lead to colorful appearances of some types of aquatic animals, birds and insects [1–3]. However, this is also a valuable resource to achieve brilliant colors and color effects by structure-engineering or other nano-technological approaches. Structural coloration appears due to light interferences with nano-sized elements and structure, and is described by optical theories including (a) multilayer interference, (b) thin-film interference, (c) Mie scattering, (d) photonic crystals or (e) localized surface plasmon resonance [4]. In contrast, pigment-based coloration is due to absorption of incident light in a specific wavelength range, which is true for most conventional dyes [5]. Investigations on naturally occurring structural coloration effects show that various repetitive structures lead to comparable, but still unique colors and color effects in wildlife. For engineered nanoscale structures, the same applies whether the colors are based on photonic crystals, nanowire-arrays or particulate structures.

While there are several ways to generate photonic or plasmonic structures on flat surfaces, creating these structures on textured substrates such as textiles is difficult and time consuming or adversely affects textile properties such as flexibility or elasticity. In recent years, this topic has received increasing attention, resulting in multiple options to generate structure-induced colors on textiles. Mainly systems made of self-assembled particulate structures have been investigated, consisting of either polystyrene-composite micro- or nanospheres, polymer-coated silicon nanoparticles, or metal nanoparticles [6–11]. These coloration methods have in common that the nanoparticles are first prepared and stabilized before application by spin-coating or spray-coating with suitable binders. While the use of metal nanoparticles also leads to antimicrobial properties, other materials only lead to coloration effects [12].

In this article, we report on a functionalization method for textiles by *in situ* growth of copper nanoparticles, which leads to coloration effects and imparts textiles with electrical conductivity that varies with the color of the fabric. The color change occurs during the deposition process and results from structural changes on fiber and fabric surfaces induced by particle formation and growth.

2 Experimental section

2.1 Materials

A desized, scoured and bleached 100% cotton fabric with mass

Address correspondence to Justus Landsiedel, Justus.Landsiedel@uibk.ac.at; Tung Pham, Tung.Pham@uibk.ac.at

109 g/m², was used as textile substrate material. The siloxane precursor (3-triethoxysilylpropyl)succinic anhydride (TESPSA, 100%) was obtained from Wacker Chemie AG, Burghausen, Germany. Tin(II) chloride dihydrate ($SnCl_2 \cdot 2H_2O$) and formaldehyde (H_3CO, 36.5 wt.%) were supplied by Riedel-de-Haen, Seelze, Germany. Copper sulfate pentahydrate ($CuSO_4 \cdot 5H_2O$, 99.5%), embittered ethanol (C_2H_6O, > 98%, MEK, 1%) and ammonia solution (NH_3, 25 wt.%) were obtained from Carl ROTH GmbH & Co. KG, Karlsruhe, Germany. Sodium carbonate (Na_2CO_3, 99 wt.%) was supplied by MERCK, Darmstadt, Germany. Silver nitrate ($AgNO_3$, 99.0 wt.%) was obtained from VWR PROLABOR, Leuven, Belgium. Sodium hydroxide (NaOH, 50 wt.% solution) was obtained from Deuring GmbH & Co. KG, Hörbranz, Austria. Potassium hydrogen-L-tartrate ($C_4H_5KO_6$, 99 wt.%) was supplied by Fluka, Buchs, Switzerland. All chemicals were used without further purification.

2.2 Preparation of siloxane coating on cotton samples

A siloxane coating was first applied on fabrics, for that an aqueous impregnation solution was prepared from 30 mmol alkoxysilane (TESPSA) and 0.5 mmol HCl in 100 mL deionized (DI) water by stirring for one hour at ambient temperature. The prehydrolyzed solution was applied on fabric samples with a two roll laboratory padder (HVL 500, Mathis AG, Switzerland) using a nip pressure on 1 bar and a roller speed of 3 m/min. The samples were then dried and heated at 180 °C for 10 min for the condensation reaction to take place. To remove any unbound siloxane deposits and other contaminants, the textile samples were thoroughly cleaned with a 1:1 (v/v) solution of DI water and ethanol.

2.3 Electroless copper deposition

The process involved three steps: (a) surface activation, (b) silver seeding, and (c) copper deposition—after each step, the samples were rinsed with DI water and dried for one hour at room temperature. For surface activation, the siloxane-coated samples were immersed for 3 min in a solution of 2.8 mmol $SnCl_2$ in 100 mL ethanol. The seeding process was carried out by immersing the activated fabrics for three minutes in a solution of 4.1 mmol $AgNO_3$ 26.6 mmol NH_3 and 100 mL DI water. For the deposition of copper, the silver seeded fabric samples were first mounted on a 2-bladed stirring blade, immersed for 5 min into a stirred solution of 2.8 mmol $CuSO_4$, 1.9 mmol Na_2CO_3, 7.9 mmol $C_4H_5KO_6$ and 24.7 mmol NaOH in 100 mL DI water. Afterwards the copper deposition was initiated by the addition of 33.6 mmol H_2CO.

2.4 Surface characterization

2.4.1 *Determination of silver and copper content*

The determination of copper and silver contents was carried out with atomic absorption spectroscopy (AAS) according to DIN 38404-18, EN-ISO 17294-2 and DIN 38406-7 on a F-AAS (contrAA 300, Analytic Jena AG, Germany) with 100 mm burner and air acetylene flame. The silver content of the samples was detected at a wavelength of 328.1 nm and the copper content at 324.8 nm. The metal content was extracted from ca. 3 cm² pieces (weighing approximately 50 mg) in a 15% (w/w) HNO_3 solution for 2 h at 80 °C. Subsequently, the solutions were filtered with a glass filter with 0.45 µm mesh size. All laboratory glassware was rinsed with HNO_3 and DI water before and after the AAS analysis.

Furthermore, to gain information about the metals and metal oxide composition present on the surface, the samples were analyzed via X-ray photoelectron spectroscopy (XPS) (Thermo MultiLab 2000 spectrometer, Thermo Fisher Scientific Inc., Waltham, USA) with an alpha 110 hemispherical analyzer, and Al K-alpha source with monochromator at 1,486.6 eV.

2.4.2 *Microscopy*

Micrographs of the colored copper-deposited textiles were taken on a stereomicroscope (SZX 16, Olympus, Tokyo, Japan) with a digital camera (XC 50, Olympus, Tokyo, Japan). The topology was investigated, with a height range of 1 to 0.1 µm, using a nano-infrared coupled atomic force microscope (NanoIR-AFM) (nanoIR2, ANASYS Instruments, Santa Barbara, USA). Further details of the surfaces were illustrated using a field-emission scanning electron microscope (FE-SEM) (JSM 7200F, JEOL, Akishima, Japan). The SEM measurements were done without deposition of any additional coating materials, using working distances between 4.8 and 5.9 mm and accelerating voltages between 2.0 and 15.0 kV. Particle sizes were measured and calculated from the FE-SEM images.

2.4.3 *Color measurement*

The color measurements (both with specular component included and excluded) were performed on a CM3610d spectrophotometer (d/8 geometry) from Konica Minolta, Japan, using an 8 mm aperture size. The values were calculated with D65 illuminant and 2° observer.

2.4.4 *Sheet resistance measurement*

The sheet resistance of the copper-coated fabrics was measured with a linear four point probe method. Current was applied on the outer points by TTi EX 1810R power supply (Thurby Thandar Instruments, Cambridgeshire, UK) and the voltage was measured on the inner points with a FLUKE 115 TRUE RMS multimeter (Fluke, Everett, USA). The measurements are related to ASTM Standards F76-2, F84-93 and F5129-94).

3 Results and discussion

3.1 Mechanism of layer formation

The method of electroless copper deposition on siloxane-based deposition templates results in the creation of uniform particulate copper structures on natural fibers. These templates are prepared in a three-step sol-gel process (Scheme 1), starting with acidic prehydrolysis of alkoxysilane (TESPSA) molecules in aqueous solution (Scheme 1(a)). The hydrolysis of the alkoxysilane molecules leads to cleavage of ethanol and formation of siloxane oligomers in solution, as well as the reaction of the anhydride unit with water to form the corresponding dicarboxylic acid groups. Impregnation of cotton textiles with the prehydrolyzed alkoxysilane solution leads to formation of siloxane films, which bind by esterification. The subsequent fixation and condensation reaction leads to the formation of a porous polysiloxane thin film with homogeneously distributed succinic acid and hydroxyl end groups (Scheme 1(b)). For electroless copper deposition, first the surfaces are activated by deposition of tin from ethanolic solution. The tin precipitates as Sn^{2+} and forms randomly arranged isles on the porous siloxane surface that are stabilized by interactions with the homogeneously distributed hydroxyl and carboxyl groups on the siloxane surface (Scheme 1(c)). Subsequently, silver seeding in form of replacement of tin species by metallic silver is performed. While the adsorbed Sn^{2+} is oxidized to Sn^{4+} in aqueous solution, the complexed Ag^+ is simultaneously reduced to metallic silver on the textile surface (Scheme 1(d)). The mechanism of copper deposition proceeds in three steps, namely the formation of electroactive species from formaldehyde in water, the reduction of copper from

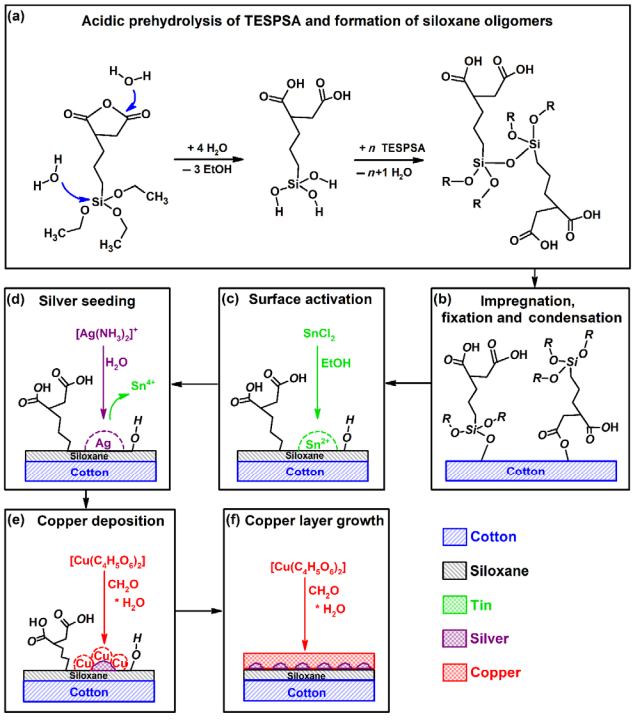

Scheme 1 Schematic procedure of the deposition of alkoxysilanes followed by electroless copper deposition.

copper(II) tartrate on the metallic silver isles that act as catalytic surfaces (Scheme 1(e)), and the growth of copper layers depending on deposition conditions (Scheme 1(f)).

During copper deposition, the carboxylic groups present in the TESPSA-based siloxane coating may serve as weak cation exchangers interfering with the tartrate complexed Cu^{2+} ions and facilitate the deposition process. In addition, the hydroxyl groups available in short distance to the carboxylates are assumed to increase the complexation probability due to stabilization effects [13]. Furthermore, a change in deposition conditions namely a shift in the pH from pH 12 to pH 8 is observed until the deposition reaction stops. While smooth copper thin-films are formed in the beginning of the reaction, particulate copper species are first observed at a pH of 10. Due to a lower deposition rate in this pH region, a more uniform growth of copper particles is proposed, which leads to the generation of color (Fig. 1).

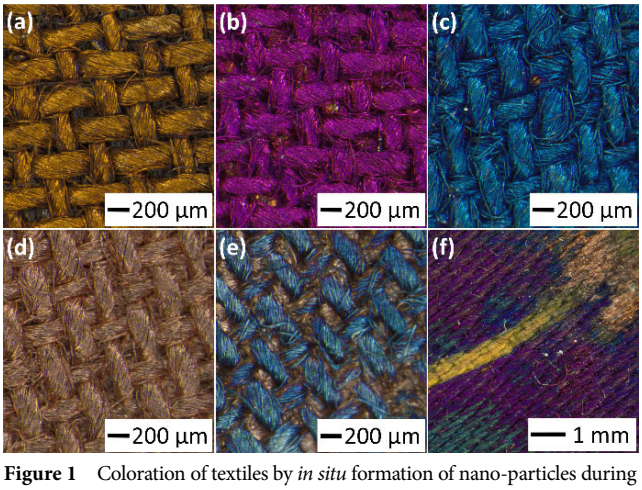

Figure 1 Coloration of textiles by *in situ* formation of nano-particles during electroless copper deposition. Controlled deposition condition lead to uniformly deposited particles, (a) 35 min—yellow, (b) 60 min—pink, (c) 70 min—blue, and (d) 90 min—copper. Uncontrolled deposition conditions regularly lead to defects on the surface, such as juxtaposed colors ((e), (f)).

3.2 Color generation

Under deposition conditions reported by Root et al. electroless copper deposition leads to the formation of coppery to brownish colored conductive surfaces on textiles [14]. However, introduction of siloxane interlayers as deposition templates and the use of defined deposition conditions results in brilliant colored surfaces with at least the same electrical conductivity. To achieve uniform metal deposition, the most critical parameters are (I) the temperature, (II) the relative motion between fabric and solution, and (III) the process time.

At temperatures below 10 °C, the deposition reaction is so slow that almost no copper deposits. In contrast, at temperatures above 25 °C, either the reaction becomes so fast that the color development is no longer controllable or alternative reactions occur. The relative motion in the deposition bath determines the diffusion rate and accessibility of the active species to the catalytic faces on the textile. High relative motion leads to successful development of colored surfaces, while lower agitation favors uncontrolled deposition on the substrate. Concentration gradients near the surface have to be maintained low by high agitation to achieve uniform rate of deposition. The deposition time to reach a specific color depends on both, the temperature and the relative motion. If these factors match properly, reproducible brilliant colors develop on the entire surface depending on the deposition time. On TESPSA coated substrates, a relative motion of 33 meter per minute and temperatures of 15 to 20 °C lead to most favorable and reproducible results. Under these conditions, the expected colors are (1) 35 to 45 min yellow to orange, (2) 45 to 55 min red to pink, (3) 55 to 65 min pink to purple, and (4) 65 to 85 min purple to blue. In Fig. 2, the progressive change in the color of samples with the process time is displayed on the CIE *xy* chromaticity coordinates. The dashed line is added as a guide to indicate increasing process times. There was a shift in the color from yellow-red towards blue. Since similar color spectra are observed in plasmonic subtractive color filtering and on reflective surfaces containing isolated particles in specific distances, a relation to LSPR is reasonable [15, 16]. Figure S1 in the Electronic Supplementary

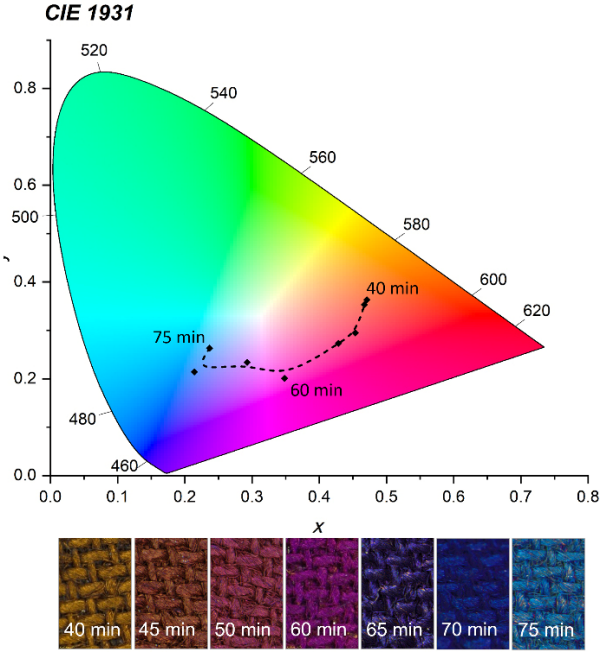

Figure 2 Color development of electroless copper deposition depending on copper deposition time shown on the CIE *xy* chromaticity coordinates. The corresponding colors are shown below the time scale. Table S1 in the ESM shows the raw reflectance data including data of aged samples.

Material (ESM) demonstrates that only minor changes in in the reflectance curves appeared after being stored at ambient conditions for six months. Further investigations on color fastness under test conditions are being undertaken in ongoing work.

3.3 Layer morphology and composition

The source of coloration was investigated via atomic force microscopy (AFM) and scanning electron microscopy (SEM) measurements (Fig. 3). Considering color generation based on e.g. localized surface plasmon resonance (LSPR), the surface layer has to meet specific parameters such as light interfering structure sizes and material compositions allowing for propagation of electromagnetic waves. While photonic coloration effects are associated with structure sizes in a range of approximately one quarter of the wavelength of incident light, nanophotonics and plasmonics are related to even smaller structure sizes [17]. AFM images of untreated and siloxane impregnated cotton textiles (Figs. 3(a) and 3(b)) reveal that the siloxane impregnation does not have a huge influence on the macroscopic structure of the substrate. No major differences are found, except for isolated adsorbed siloxane-clusters possibly build up during prehydrolysis of the solution. By deposition of silver, no continuous layer, but additional small isolated clusters are formed on the fiber surface [18].

In contrast, after copper deposition, the surfaces show macroscopic repetitive surface features describable as ridges and valleys with diameters of up to several hundred nanometers in extent (Fig. 3(c)). Therefore, the arising structures are assumed to be dependent on the distribution of silver and the

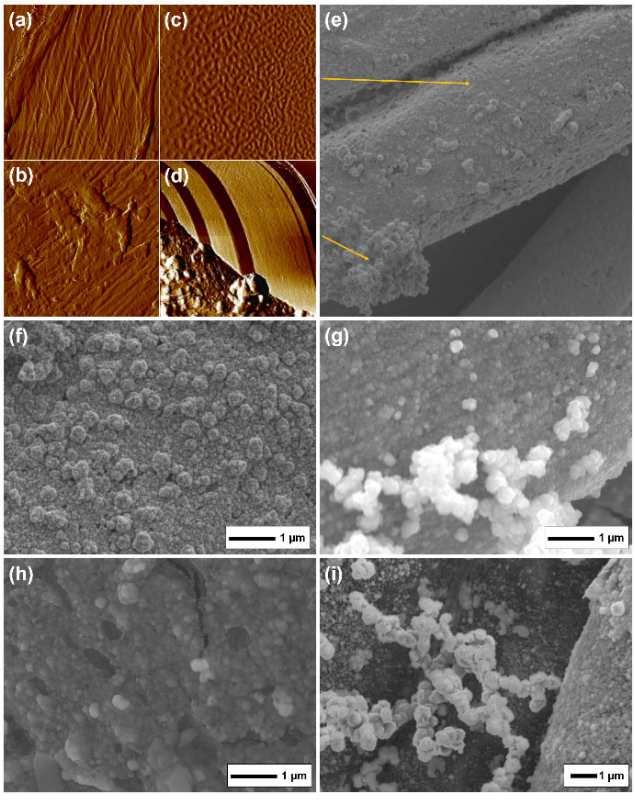

Figure 3 Topological investigation of (a) raw cotton, (b) siloxane-deposited cotton, ((c) and (d)) siloxane and copper deposited cotton samples via AFM (7 μm × 7 μm, deflection images). Surface investigation of (e) purple colored copper sur-face in 6,500× magnification, (f) red copper surface after 45 min, (g) purple copper surface after 60 min, (h) blue surface after 75 min copper deposition in 18,000× magnification, and (i) coppery surface of a reference sample without siloxane pretreatment in 10,000× magnification.

growth rates on the different substrate species. A change in morphology is observable with increasing copper deposition time. By visualizing the surface features by means of SEM, the repetitive structures gained by copper deposition (Fig. 3(c)), are identified as pores and particles (Fig. 3(e)). Also the bumps visible in (Fig. 3(d)) show similarities to adsorbed clusters seen in the SEM image. These surface features may arise from continuous copper deposition and growth of the structures. At higher magnifications, SEM images reveal that fiber surfaces are densely packed with particles (primary particles) and agglomerates (secondary particles). For each sample, the primary particles show only small differences in size, while the size of the secondary particles varies in a range of several hundred nanometers. By comparison of the surface features on fibers of a red, purple and blue colored textile (Figs. 3(f)–3(h)), time dependent formation of parent structures by *in situ* growth of particles is assumed. Figure 3(i) shows the surface of a copper coated reference sample that was produced without the use of siloxane interlayers. The particle sizes on this sample vary significantly. In particular, the image of the red sample (Fig. 3(f)) gives the impression of the formation of nanoparticle-based layers and the growth of agglomerates on top. While the mean diameter of the primary particles increases from 35 nm at a deposition time of 40 min to 80 nm at a deposition time of 75 min, there is no observable trend for the formation and growth of secondary particles (Table 1). Considering several features such as particle-to-particle distances, particle shapes and environmental effects, the particle sizes found on the surface of these samples are in agreement with the requirements for the excitation of surface plasmons for the LSPR mechanism [19, 20].

The composition of the deposited copper layers were analyzed via AAS and XPS. The AAS measurements show a consistent silver amount for all samples, as well as an increase in copper content with process time. That correlates with the increase in particle size and the color change (Table 1). The XPS measurements were performed since the limited penetration depth of the analysis (of a few nanometers) which allows the determination of the material composition at the surface of samples (Fig. 4). Figure 4(a) shows very similar profiles for all differently colored copper-coated textiles.

Differences seen in the Cu2p region (Fig. 4(b)) and in the Cu Auger region (Fig. 4(c)) were compared to NIST database [21]. In the Cu2p region, copper(I) oxide and copper metal are most evident due to peaks at 932.4 and 952.2 eV, but also lower amounts of copper(II) oxide are found with peaks at 934.7 and 954.0 eV. Strong Cu^{2+} satellite peaks at 944.0 and 964.0 eV are not seen. The Cu Auger region shows clear evidence for the formation of a passivation layer made of copper(I) oxide by the peak at 916.8 eV, as well as the peak-peak distance of 1.8 eV of copper(I) oxide to metallic copper peak maximum at 918.6 eV after ablation of approximately 1.9 nm from the surface. Since the results from all representative samples were similar, we concluded that the color differences between samples did not arise from changes in the coating composition or the layer thickness. It is known that nanoparticle clusters exhibit different colors as compared to isolated nanoparticles, and that the surface on which nanoparticles rest also exerts an influence—both are attributed to interference effects in the plasmonic resonance of the nanoparticles. The XPS analyses revealed the presence of a passivation layer of Cu_2O, which may act as a dielectric and change the physical environment of the copper and thereby the plasmon resonance [22]. Thus, the colors generated in our experiments appear to be the result of all these effects.

Table 1 Interrelation of color, deposition time, material composition, structural information and average sheet resistance of the samples

Color and deposition time (min)	Ag content (mg/g)	Cu content (mg/g)	Primary particle size (nm)			Secondary particle size (nm)			Average sheet resistance (Ω/square)
			min	max	average	min	max	average	
Red (40)	18.6 ± 0.3	159.1 ± 2.4	30	43	35 ± 4	117	394	250 ± 79	3.23 ± 0.22
Purple (60)	20.4 ± 0.5	170.1 ± 2.4	47	83	58 ± 8	141	375	241 ± 46	0.93 ± 0.09
Blue (75)	18.0 ± 0.2	174.5 ± 3.1	66	97	80 ± 9	208	531	317 ± 85	0.57 ± 0.03
Reference (72) [14]	31.3 ± 17.8	151.5 ± 4.2	93	168	121 ± 22	187	748	381 ± 146	16.53

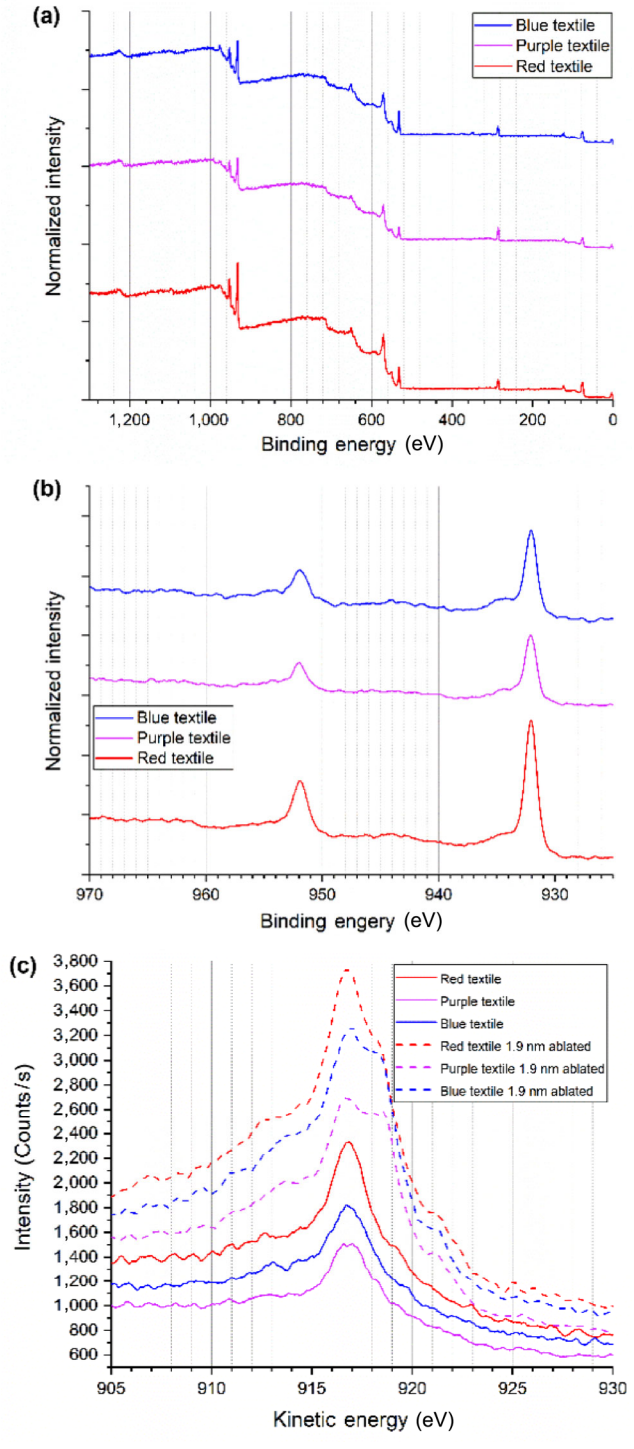

Figure 4 XPS data for three differently colored textiles, red, purple and blue. In (a) the survey, (b) the Cu2p and (c) Cu(LMM) spectra only minor differences between the samples composition are seen. Ablation of approximately 1.9 nm from the surface reveals the core-shell-structure of the passivated copper/copper oxide particles.

3.4 Electrical conductivity

The quality of thin conductive coatings is characterized by the sheet resistance and depends on the thickness and the continuity of the coating. Since conductive coatings formed by electroless metal deposition consist of self-assembled metal particles, the conductivity is related to the connectivity of the particles and the number of particle boundaries that may scatter electrons [23]. In the case of electroless copper deposition on siloxane-coated textiles, the quality of the conductive layer is also indicated by the color of the surface, as displayed in Table 1. Since samples in red color consist of many small copper particles with diameters of approximately 35 nm, there are many particle boundaries. Boundaries between particles may hinder the current flow, which leads to large sheet resistances of approximately 3.2 Ω/square.

In contrast, the blue samples that are formed of particles in approximately doubled size, show average sheet resistances of 0.57 Ω/square, which supports the theory of better electrical conductivity due to higher connectivity of the particles and less particle boundaries. This theory is further confirmed by the small mass increase of copper from a red to a blue colored textile, which is approximately 10%. By comparing the colored copper-coated samples with a reference sample that was produced without siloxane deposition templates, the dependency between uniformity of the coating indicated by the consistent colors and the gain in electrical conductivity becomes more obvious (Fig. 5). Variations in particle sizes on self-assembled particle-based surfaces lead to imperfections in the sheet, which reduce the connectivity while the layer thickness increases. The lowest sheet resistance of 0.57 Ω/square of the copper layer was obtained at an average particle size of 80 nm, which is observed at copper contents of approximately 174.5 mg/g sample.

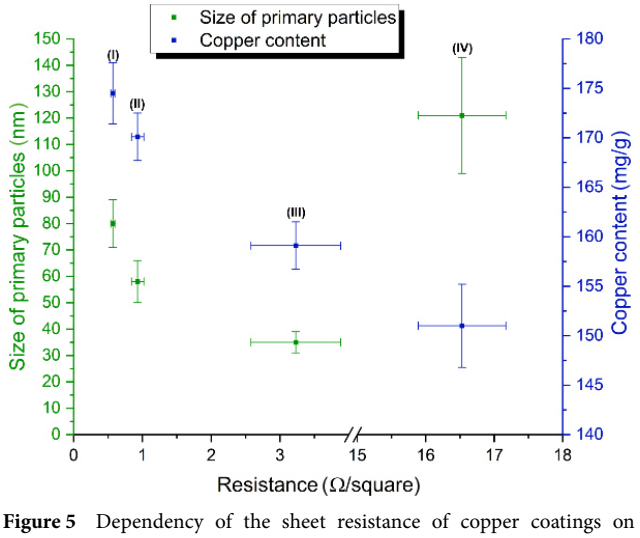

Figure 5 Dependency of the sheet resistance of copper coatings on particle sizes and copper content. Left to right: (I) blue sample, (II) purple sample, (III) red sample, (IV) reference sample.

4 Conclusion

Sol-gel supported electroless copper deposition opens a new promising strategy for controlled functionalization and coloration of non-conductive substrates. The three-step procedure consists of alkoxysilane based sol-gel surface modification, followed by deposition of silver seeds for the subsequent growth of Cu/Cu_2O core-shell particles by electroless deposition of copper. The siloxane-based interlayer acts as an adhesion promotion layer and as a structured deposition template for the metal deposition. The adhesion promotion is assumed to be related to Si-O/Cu interactions and the dicarboxylic function of the alkoxysilane precursor with the cellulose substrate. The core-shell structure of the Cu/Cu_2O particles was confirmed by XPS measurements, and was attributed to the surface oxidation during the rinsing and drying operations performed after the deposit formation. Depending on the structure of the copper layer arising on the interlayer, a wide color spectrum including diverse colors with different shades is observed apart from the colors of copper oxides, namely yellow, red and black. Thus, we conclude that the color development is attributed to physical effects based on the structure, the particle size, the particle distributions, and the related changes in inter-particle distances. Therefore, a relation between the effects seen on the nano-structured coating and light-interference based on LSPR mechanism seems most reasonable. As an example, surfaces showing particles with average diameter of 35 nm developed red color, while surfaces showing particles with 80 nm average diameter led to generation of blue color. Interestingly, a correlation between the color of the deposited surface layer and the electrical conductivity was found. Based on the measured sheet resistances, the specific electrical resistances were estimated to be 1,200 μΩ·cm for yellow colored textiles, 300 μΩ·cm for red colored textiles, 100 μΩ·cm for purple colored textiles and 50 μΩ·cm for blue colored textiles. The higher conductivity of the sol-gel treated samples is due to a more uniform distribution of the silver seeds and copper particles on the surfaces of the fibers. The colors of the samples have been stable for over six months of storage at ambient conditions. Thorough investigations on color fastness are being undertaken in ongoing work.

The present sol-gel based electroless copper deposition technique is applicable on different materials and types of substrates. Multiple conditions can still be adapted and optimized for a transfer of the process in larger scale. Thus, the process can be considered as a powerful tool for the surface modification and functionalization towards structure-based coloration and formation of conductive surface layers with well-defined appearances.

Acknowledgements

The authors gratefully acknowledge the financial support from the Austrian Federal Ministry for Climate Action, Environment, Energy, Mobility, Innovation and Technology (BMK) for the Endowed Professorship Advanced Manufacturing (No. 846932), and the BMK, BMWFW, Land Vorarlberg, Land Tirol and Land Wien with the framework of COMET competence Centers for Excellence Technologies for the K-Project TCCV (No. 860474). J. L. thanks Dr. Avinash P. Manian and Dr. Noemí Aguiló-Aguayo for discussions, and Dorian Rhomberg for laboratory support.

Funding note: Open access funding provided by University of Innsbruck and Medical University of Innsbruck.

Electronic Supplementary Material: Supplementary material (Fig. S1: indication on the color stability; Table S1: raw reflectance data of samples shown) is available in the online version of this article at https://doi.org/10.1007/s12274-020-2907-5.

References

[1] Vukusic, P.; Noyes, J. Photonic structures in nature. In *Bionanotechnology II*. Reisner, D. E., Ed.; CRC Press: Boca Raton, 2011; pp 497–517.

[2] Srinivasarao, M. Nano-optics in the biological world: Beetles, butterflies, birds, and moths. *Chem. Rev.* **1999**, *99*, 1935–1962.

[3] Rosenthal, E. I.; Holt, A. L.; Sweeney, A. M. Three-dimensional midwater camouflage from a novel two-component photonic structure in hatchetfish skin. *J. Roy. Soc. Interface* **2017**, *14*, 20161034.

[4] Kinoshita, S.; Yoshioka, S.; Miyazaki, J. Physics of structural colors. *Rep. Prog. Phys.* **2008**, *71*, 076401.

[5] Zollinger, H. *Color Chemistry*: *Syntheses*, *Properties*, *And Applications of Organic Dyes and Pigments*; Weinheim: New York, 2003.

[6] McGrath, J. G.; Bock, R. D.; Cathcart, J. M.; Lyon, L. A. Self-assembly of "paint-on" colloidal crystals using poly(styrene-co-*N*-isopropylacrylamide) spheres. *Chem. Mater.* **2007**, *19*, 1584–1591.

[7] Shao, J. Z.; Zhang, Y.; Fu, G. D.; Zhou, L.; Fan, Q. G. Preparation of monodispersed polystyrene microspheres and self-assembly of photonic crystals for structural colors on polyester fabrics. *J. Text. Inst.* **2014**, *105*, 938–943.

[8] Zeng, Q.; Ding, C.; Li, Q. S.; Yuan, W.; Peng, Y.; Hu, J. C.; Zhang, K. Q. Rapid fabrication of robust, washable, self-healing superhydrophobic fabrics with non-iridescent structural color by facile spray coating. *RSC Adv.* **2017**, *7*, 8443–8452.

[9] Liu, P. M.; Chen, J. L.; Zhang, Z. X.; Xie, Z. Y.; Du, X.; Gu, Z. Z. Bio-inspired robust non-iridescent structural color with self-adhesive amorphous colloidal particle arrays. *Nanoscale* **2018**, *10*, 3673–3679.

[10] Elmaaty, T. A.; El-Nagare, K.; Raouf, S.; Abdelfattah, K.; El-Kadi, S.; Abdelaziz, E. One-step green approach for functional printing and finishing of textiles using silver and gold NPs. *RSC Adv.* **2018**, *8*, 25546–25557.

[11] Shahid-Ul-Islam; Butola, B. S.; Mohammad, F. Silver nanomaterials as future colorants and potential antimicrobial agents for natural and synthetic textile materials. *RSC Adv.* **2016**, *6*, 44232–44247.

[12] Dastjerdi, R.; Montazer, M.; Shahsavan, S. A new method to stabilize nanoparticles on textile surfaces. *Colloids Surf. A Physicochem. Eng. Asp.* **2009**, *345*, 202–210.

[13] Emam, H. E.; Manian, A. P.; Široká, B.; Bechtold, T. Copper inclusion in cellulose using sodium D-gluconate complexes. *Carbohydr. Polym.* **2012**, *90*, 1345–1352.

[14] Root, W.; Aguiló-Aguayo, N.; Pham, T.; Bechtold, T. Conductive layers through electroless deposition of copper on woven cellulose lyocell fabrics. *Surf. Coat. Technol.* **2018**, *348*, 13–21.

[15] Kristensen, A.; Yang, J. K. W.; Bozhevolnyi, S. I.; Link, S.; Nordlander, P.; Halas, N. J.; Mortensen, N. A. Plasmonic colour generation. *Nat. Rev. Mater.* **2017**, *2*, 16088.

[16] Hu, X. L.; Sun, L. B.; Zeng, B. B.; Wang, L. S.; Yu, Z. G.; Bai, S. A.; Yang, S. M.; Zhao, L. X.; Li, Q.; Qiu, M. et al. Polarization-independent plasmonic subtractive color filtering in ultrathin Ag nanodisks with high transmission. *Appl*. *Opt*. **2016**, *55*, 148–152.

[17] Fan, X. F.; Zheng, W. T.; Singh, D. J. Light scattering and surface plasmons on small spherical particles. *Light Sci*. *Appl*. **2014**, *3*, e179.

[18] Root, W.; Wright, T.; Caven, B.; Bechtold, T.; Pham, T. Flexible textile strain sensor based on copper-coated lyocell type cellulose fabric. *Polymers (Basel)* **2019**, *11*, 784.

[19] Noguez, C. Surface plasmons on metal nanoparticles: The influence of shape and physical environment. *J*. *Phys*. *Chem*. *C* **2007**, *111*, 3806–3819.

[20] Fan, P. X.; Zhong, M. L.; Li, L.; Schmitz, P.; Lin, C.; Long, J. Y.; Zhang, H. J. Angle-independent colorization of copper surfaces by simultaneous generation of picosecond-laser-induced nanostructures and redeposited nanoparticles. *J*. *Appl*. *Phys*. **2014**, *115*, 124302.

[21] Naumkin, A. V.; Kraut-Vass, A.; Gaarenstroom, S. W.; Powell, C. J. *NIST X-Ray Photoelectron Spectroscopy Database* [Online]. https://srdata.nist.gov/xps/ (accessed Mar 2, 2020).

[22] Haynes, C. L.; Van Duyne, R. P. Nanosphere lithography: A versatile nanofabrication tool for studies of size-dependent nanoparticle optics. *J*. *Phys*. *Chem*. *B* **2001**, *105*, 5599–5611.

[23] Cui, X. Y.; Hutt, D. A.; Conway, P. P. Evolution of microstructure and electrical conductivity of electroless copper deposits on a glass substrate. *Thin Solid Films* **2012**, *520*, 6095–6099.